frontiers | Frontiers in Earth Science

TYPE Original Research
PUBLISHED 03 August 2023
DOI 10.3389/feart.2023.1188602

OPEN ACCESS

EDITED BY
Ziyadin Cakir,
Istanbul Technical University, Türkiye

REVIEWED BY
Alessandro Maria Michetti,
University of Insubria, Italy
Maria Francesca Ferrario,
University of Insubria, Italy
Yosuke Aoki,
The University of Tokyo, Japan

*CORRESPONDENCE
P. Galli,
paolo.galli@protezionecivile.it

RECEIVED 17 March 2023
ACCEPTED 19 July 2023
PUBLISHED 03 August 2023

CITATION
Galli P, Messina P, Peronace E, Galderisi A, Ilardo I and Polpetta F (2023), Paleoseismic evidence of five magnitude 7 earthquakes on the Norcia fault system in the past 8,000 years (Central Italy). *Front. Earth Sci.* 11:1188602. doi: 10.3389/feart.2023.1188602

Paleoseismic evidence of five magnitude 7 earthquakes on the Norcia fault system in the past 8,000 years (Central Italy)

P. Galli[1,2]*, P. Messina[2], E. Peronace[2], A. Galderisi[2], I. Ilardo[3] and F. Polpetta[2]

[1]Dipartimento Protezione Civile, Rome, Italy, [2]Consiglio Nazionale delle Ricerche, Istituto di Geologia Ambientale e Geoingegneria, Rome, Italy, [3]Freelance Geologist, Rome, Italy

Many large-magnitude faults (6.5≤ Mw ≤7.2) of the Italian Apennines are characterized by multi-century return times, so historical sources may have missed their last earthquake or other predecessors. Hence, even in Italy, where seismic catalogs are among the most comprehensive and time-extensive worldwide, there is a need for complementary studies that might fill the lack of historical information and enhance the knowledge concerning the recurrence times of destructive earthquakes. As paleoseismology is the discipline that can do this, in this study, we present results collected in five new trenches opened along the 33-km-long Norcia fault system (central Apennines) where, in addition to the historically known 1703 earthquake (Mw 6.9), we uncovered indications of four Holocene predecessor, with a recurrence time of 1,825 ± 420 years. Considering also the paleoseismic results already published on the nearby Mt Vettore fault system (2016 earthquake of Mw 6.6), we guess that now the seismic hazard of this region could be assessed more robustly.

KEYWORDS

paleoseismology, active tectonics, recurrence time, fault interaction, Central Italy

1 Introduction

Although the Italian seismic catalogs are probably among the most comprehensive and time-extensive compilations worldwide, the recurrence times of destructive earthquakes (Mw ≥6.5) throughout the seismogenic structures of the Apennines are sometimes longer or at the limit of the time span covered by historical sources (Galli, 2020). For this reason, it is likely that we missed more than a few strong earthquakes between the Roman times and the end of the Middle Ages (e.g., in Stucchi and Albini, 2000). Thus, extending seismic catalogs back in time to include at least the last missing events released by a silent fault or the predecessors of an earthquake known to have been sourced by a seismogenic structure is the challenge for the next-generation of earthquake geologists in Italy.

A recent case is the rupture of the Mt Vettore normal fault (2016 central Italy sequence: Mw 6.2, Mw 6.1, Mw 6.6; Figure 1), a historically dormant structure for which three paleoseismic trenches opened in February 1998 (Galli and Galadini, 1999) had already identified, among others, the last two paleoearthquakes and, in particular, the ultimate Mw 6.6 event that occurred just before 240–480 CE (Galadini and Galli, 2003). Further paleoseismic studies have now refined the age of the 2016 predecessor

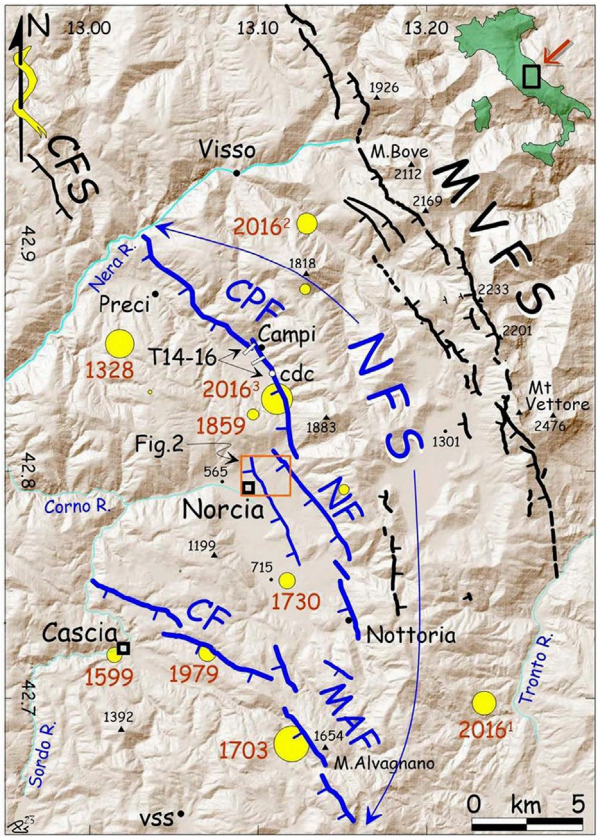

FIGURE 1
Shaded relief map of the region traversed by the Norcia fault system (blue lines, NFS. CPF, Campi-Preci segment; NF, Norcia segment; MAF, Mount Alvagnano segment; CF, Cascia faults) and by the Mount Vettore fault system (black, MVFS). CFS, the southernmost tip of the Colfiorito fault system. Yellow circles, epicenters of Mw≥5.5 events (mod. from CPTI15, 2015). MVFS was responsible for the three mainshocks of the 2016 seismic sequence, labeled 2016[1–3]. Orange box, Figure 2; cdc, Capo del Colle. Modified from Galli et al. (2022).

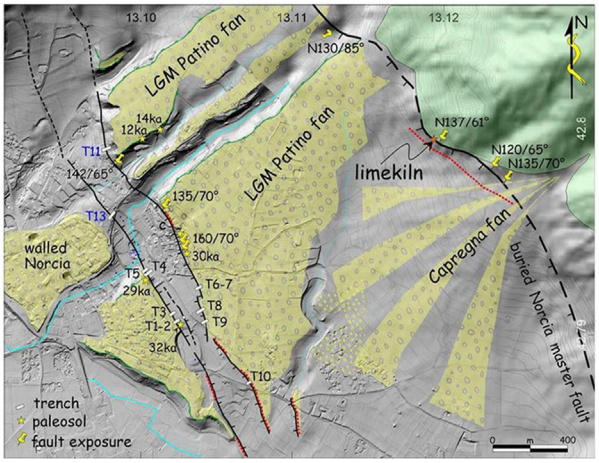

FIGURE 2
Shaded relief map of the Norcia area (see orange rectangle in Figure 1 for location) evidencing the faulted, relic top-surface (yellow) of the Late Pleistocene-post Last Glacial Maximum (>14–12 ka) alluvial fan of Patino (stars, 14C dated paleosols within the Patino fan gravels). Note the NW-SE Graben-like structure that downthrows the distal sector of this fan (left), and the Norcia master fault traversing its medium portion (upper-right). T1-10 are the paleoseismological trenches in Galli et al. (2018), T11 and T13 in this paper. Green, Meso-Cenozoic, marine carbonates. Gray, other Quaternary slopes, and alluvial deposits (Middle Pleistocene-Holocene). Red dotted lines indicate the 2016, passive fault re-activation (Galderisi and Galli, 2020).

(Galli et al., 2019), associating it with the 443 CE earthquake, which is already on record in the catalogs although with an epicenter in Rome and an unreliable magnitude (Mw 5.6; CFTI5Med, 2018). If these paleoearthquakes had been considered with the right epicentral parameters provided by the studies of the late 1990s, we imagine that the framework of the seismic hazard of the region would have been different, as well as the awareness of the associated seismic risk.

We present in this study the results gathered from five new paleoseismic trenches opened across the 33-km-long Norcia fault system (Figure 1), which is a normal structure roughly paralleling the Mt Vettore fault in its hanging wall, and that was responsible for the Mw 6.9 event that occurred on 14 January 1703. Our results integrate those obtained from 10 previous trenches that we opened in the Norcia surroundings, as well as other key outcrops that were re-excavated and investigated along different segments of the fault system.

2 Seismotectonic framework

2.1 Historical seismicity

The seismicity of the Norcia region over the past millennium is fairly well known, with some reports for earlier periods as well. Like most Italian settlements, Norcia has its roots in the mists of time so that underneath the remains of the Roman municipium, archaeologists discovered a palimpsest of older settlements, extending back to the Bronze Age (12th century BCE; e.g., in Fazzini et al., 2001). The first accounts of an earthquake in Norcia date back to Roman times (99 BCE) when because of a "terrae motu" the sacred temple was destroyed (see details in Galli et al., 2018). Archaeological investigations in the surrounding region have confirmed the energy of this event, providing indications of structural damage and collapse of Roman buildings datable to the onset of the first century BCE (Coarelli and Diosono, 2009; Galli, 2023). Similar to all the Mw >6 Apennine earthquakes, this event was strongly felt in Rome (120 km away), where Mars' spears trembled in the Regia (see Galli and Molin, 2014). Although historical sources remained silent for more than a millennium, we again have information about strong earthquakes in the last seven centuries (see macroseismic epicenters in Figure 1). The first one destroyed Norcia (site intensity: Is 9–10 MCS; Mercalli-Cancani-Sieberg scale, Sieberg, 1932) and other neighboring settlements on 4 December 1328 (Mw ~ 6.5) with approximately a thousand of victims. Another one, in 1599 (Mw ~ 6.0), struck all

the villages of the Cascia basin, with 50 victims. Then, a catastrophic earthquake occurred on 14 January 1703 (Io, 11 MCS; Mw ~ 6.9), when Norcia and dozens of villages in the whole region were literally razed to the ground (site intensity Is 10–11 MCS) and again strong effects were reported in Rome (Galli and Molin, 2014). According to a contemporary physician (Baglivi, 1710), during the mainshock, "prominent chasms opened in the Norcia fields," which suggests the occurrence of extensive surface faulting. The same was reported for the hillslope of Mt Alvagnano that opened "for a length of 1.5 miles" (i.e., 2.2 km; De Carolis and Franceschini, 1703; De Carolis, 1703; or "for the length of 1,500 paces"; Baglivi, 1710) and further to the south, "for a length of 1.5 miles" (Baglivi, 1710). In 1730, an Mw ~ 6.0 earthquake hit the region again with severe damage in Norcia (Is 9 MCS, 200 victims in Norcia), while in 1859, an Mw ~ 5.7 event caused new damage to many settlements in the Campi basin, with effects of Is 8–9 MCS in Campi and Norcia, where 101 person died due to the collapse of several buildings. In 1979, a Mw 5.9 twin of the 1599 event induced macroseismic effects of Is 8–9 MCS in the Cascia basin and Is 7 MCS in Norcia, where faint ground breaks were observed as well as along the Mount Alvagnano-Civita slopes (Marsan and Cerone, 1980; Blumetti, 1995).

In the end, the 2016 sequence (Mw 6.2–6.1–6.6), generated by the progressive rupture of the Mt Vettore fault system (MVFS, Figure 1), caused the collapse of all the churches in Norcia and Campi as well as most of the villages of the area, besides severe damage and collapses to many buildings. Note worthily, some urban splays of the Norcia fault recorded up to 12 cm of surface offset (red dotted lines in Figure 2; Galderisi and Galli, 2020) although no earthquakes were released by this fault (Improta et al., 2019).

2.2 Active tectonics

Active tectonics in the Italian Apennines is driven by NW-SE striking normal faults, roughly aligned along the entire divide of the chain (Galadini and Galli, 2000) and accommodating 2.9–3.4 mm/year NE-SW extension (D'Agostino, 2014; Devoti et al., 2017). Since the Late Pliocene, these faults have progressively dissected the pre-existing Apennine fold-and-thrust wedge, giving rise to a peculiar morphology consisting of elongated intramontane basins that developed in their hanging wall and were increasingly filled by Quaternary fluvial-to-lacustrine deposits (Cinque et al., 1993; Bosi et al., 2003; Boncio et al., 2004; Galadini and Messina, 2004; Galli et al., 2010; Giaccio et al., 2012), with sedimentation rates proportional to fault slip rates (Giaccio et al., 2023).

The Quaternary evolution of the Norcia region has been investigated by many authors (e.g., Scarsella, 1941; Calamita et al., 1982; Blumetti and Dramis, 1993; Brozzetti and Lavecchia, 1994; Calamita et al., 1994; Calamita et al., 1995; Cello et al., 1997; Galadini and Galli, 2000; Galli et al., 2020; ISPRA, 2021). These studies, integrated with paleoseismic investigations, allowed for the identification of the branched Norcia Fault System (NFS; Figure 1) as the seismogenic structure responsible for most of the historical seismicity of the region (Galli et al., 2005; Galli et al., 2018; Galli et al., 2020). The 33-km-long NFS is composed of three main NNW-SSE normal faults with dextral step-over (from the north: Campi-Preci, Norcia, and Cascia-Mt Alvagnano; Figure 1), running 10 km away from the Mt Vettore fault system, in its hanging wall. The segments are characterized by rectilinear slopes, triangular facets, and wine-glass valleys along the eastern carbonate hillslopes of as many elongated intermontane basins (Figure 3). Some of these basins are still in an embryonic phase (e.g., Mt Alvagnano segment), while others are filled with Middle-Late Pleistocene fluvial-lacustrine deposits, rich in tephra levels that allowed K/Ar dating of a part of the alluvial succession (e.g., in ISPRA, 2021). The long-term activity of the NFS can also be inferred from numerous evidence of Early to Middle Pleistocene-faulted slope-breccias outcropping along the entire fault system, as well as Middle Pleistocene alluvial deposits displaced by secondary faults within the Norcia basin (Blumetti and Dramis, 1993). As aforementioned, the Late Pleistocene activity of these faults has been ascertained by several paleoseismological studies conducted over the past 20 years. In particular, since the early 2000s, a pair of secondary splays running in the hanging wall of the Norcia master fault (herein referred to as urban splays of Norcia) have been investigated by 10 paleoseismological trenches (Figure 2). Trenches 1-3 were opened in 2003 across the antithetic splay (Galli et al., 2005), as well as trenches 4-5 in 2005. Trenches 6-7 in 2005 and 8-9 in 2006 were opened across the synthetic splay, as was Trench 10 in 2017. Data and results are summarized in Galli et al. (2018). Additional paleoseismological evidence was found along the Cascia-Monte Alvagnano segment (Galli et al., 2020), as well as from an awesome archaeoseismic case point on the Norcia master fault (Galli et al., 2022). In contrast, no evidence of recent surface faulting has ever been found along the Preci-Campi segment. Overall, in the 10 trenches opened across the Norcia urban splays, Galli et al. (2018) found indications for two other paleoearthquakes in addition to the 1703 earthquake. One matching the historically known 99 BCE event and one occurring earlier in the first half of the second millennium BCE at the beginning of the Middle Bronze Age (i.e., just before 3,600–3,800 BP). Besides these three consecutive earthquakes, an earlier event has been dated to around 7,500 BP.

3 Materials and methods

3.1 Field investigations

Field investigations were carried out in the area crossed by the NFS in both Norcia and Campi basins. Geological, structural, and sedimentary-facies analyses were integrated with field geomorphological observations and aerial stereopair photos (1954 NATO photographs; 1:33,000 scale), together with a digital terrain model (DTM) that we derived from 1:5,000 topographic maps and, partly, from a 1-m resolution LiDAR DTM (Norcia basin).

3.2 Paleoseismic trenches

Five paleoseismic excavations were carried out using different tracked diggers. After digging, the exposed walls were cleaned, smoothed, and equipped with a 0.5 to 1-m-spaced grid, and then plotted at a 1:20 scale on a millimeter graph paper. Hundreds of georeferenced photos were taken with different natural and artificial

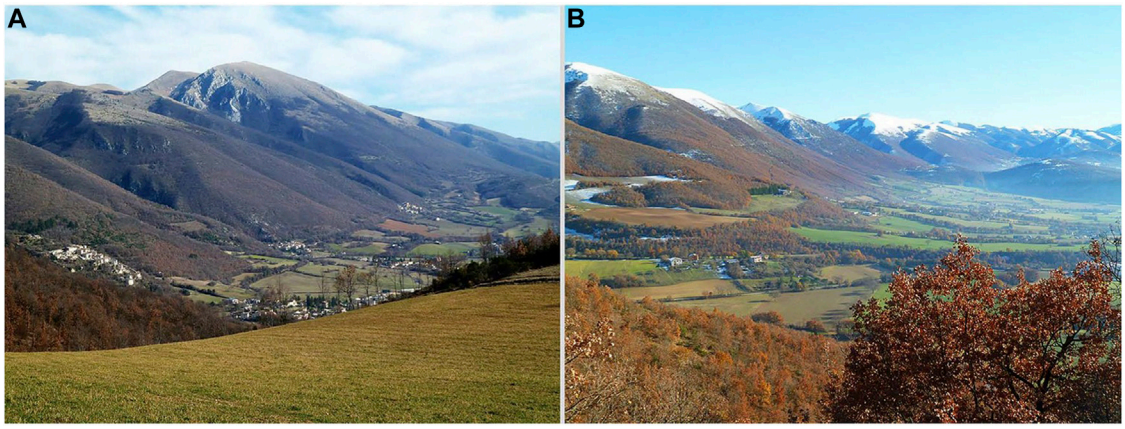

FIGURE 3
View looking southeast of the Campi **(A)** and Norcia **(B)** intramontane basins, both bounded on their eastern side by a flat, rectilinear fault-slope, with triangular facets and wine-glass valleys. The carbonate slickenside is almost completely buried by thick talus deposits in the Norcia basin, whereas it outcrops discontinuously in the Campi basin.

light and then mosaiced and overlaid on the final trench plot. High-detail photomosaics of the trench walls were created based on a workflow from Reitman et al. (2015) and Delano et al. (2021), using Structure-from-Motion (SfM) algorithms by AgiSoft Metashape software. In one trench, the presence of loose deposits caused the instability of the walls, resulting in repeated detachments of sediment slices that made it impossible for the continuous and detailed survey of the trench. Therefore, the complete investigation of the walls was conducted using an IOS-based laser scanner (IPad Pro) and through a photo-mosaic, while the topographic references (scarp and trench profile, network vertices, samples, and key horizons) were obtained with a GNSS RTK satellite receiver. Samples of organic sediments (paleosols and colluvia), charred materials, bones, and ceramic materials (bricks and tiles) were also collected for dating the different stratigraphical units.

3.3 Dating

The age of the deposits has been constrained by both radiocarbon analyses (see Table 1) and chronologically diagnostic archaeological pottery shards. The latter was studied following the procedures and literature reported for the same aim by Galli et al. (2005). The former was performed on both detrital charcoals and bulk samples using the accelerator mass spectrometry (AMS) technique at the Beta Analytic (Miami, United States) laboratories. Standards and analytical protocols are both available at http://www.radiocarbon.com/.

4 New results

Two trenches were opened across the Norcia urban splays: trench#11 across the fault scarp cumulated by the synthetic fault and trench#13 across the antithetic one, close to the Roman-Medieval walls of Norcia (T11 and T13 in Figure 2). The other three trenches were opened across the Campi segment: trench#14 in Capo del Colle (T14; cdc in Figure 1), a medieval settlement built just above the fault slickenside and trenches#15 and #16 at the apex of two alluvial fans exiting the fault hillslope south and north of Campi (T15 and T16 in Figure 1). These were the first trenches ever excavated on the Campi segment.

4.1 Trench 11 (Norcia synthetic splay)

This 50-m-long and 4-m-deep trench was designed across the synthetic splay that traverses the northeastern outskirts of Norcia, approximately 1.5 km downward the master fault (Figure 2). This splay caused up to 35 m offset of the top surface of the Patino alluvial fan, as measured in different profiles across the resulting 1.5-km-long fault scarp. At the base of the scarp, Galli et al. (2005), Galli et al. (2008), Galli et al. (2018), Galli et al. (2022) report rare outcrops of the hardened fault plane affecting the alluvial fan deposits, as well as several interbedded paleosols dated between 30 and 12 ka.

4.1.1 Stratigraphy

In the footwall, below the present-day pedogenetic horizon (unit 1 in Figure 4), the excavation unearthed faintly stratified carbonate gravels, with interbedded 10–20 cm-thick subhorizontal paleosols (unit 6, distal portion of Late Pleistocene-Holocene Patino alluvial fan). Two AMS ages of these paleosols (13 and 18 ka) match those of other paleosols sampled in natural outcrops next to this site (Figure 4; Galli et al., 2022). Approaching the main fault, a set of synthetic and antithetic shear planes makes it very complicated to draw the limit between the original alluvial fan succession and its reworked material. These shear planes have been superimposed by tensile fractures that were successively filled by other colluvia and then notched by anthropic pits infilled by coarse, rounded gravels (4a). Upward, all is mantled by a brownish colluvium (2) deposited above an erosional surface. Conversely, the hanging wall presents only gravelly colluvia in the abundant, sandy, reddish matrix, organized in thick massive bodies paralleling the slope profile

TABLE 1 Radiocarbon ages of samples collected in the investigated area in this study and previous studies (AMS, accelerator mass spectrometry by Beta Analytic Inc., Florida). 2σ calibration with software CALIB 8.2 software (Stuiver et al., 2021). G&18, Galli et al. (2018); G&22, ISPRA21, ISPRA (2021); Galli et al. (2022).

Trench/Site	Sample	Lab code	Analysis	Dated material	δ13C	Conventional age (BP)	2σ cal. 95%	Reference
T11	TR01-C01	BETA-630856	AMS	Charred material	−25.1	400 ± 30	1,435–1,625 CE	This study
	TR01-CW01	BETA-630855	AMS	Organic sediment	−23.3	6,660 ± 30	7,585–7,435 BP	This study
	TR01-PS01	BETA-630854	AMS	Organic sediment	−23.7	11,100 ± 40	13,100–12,910 BP	This study
	TR01-PS02	BETA-630853	AMS	Organic sediment	−24.2	14,980 ± 40	18,600–18,590 BP	This study
	NOR11-05	BETA-630852	AMS	Organic sediment	−24.1	520 ± 30	1,395–1,445 CE	This study
	NOR11-07	BETA-630851	AMS	Charred material	−24.7	220 ± 30	1,640–1,805 CE	This study
	NOR11-06	BETA-630850	AMS	Organic sediment	−24.2	780 ± 30	1,220–1,280 CE	This study
Patino Fan	TOPATINO01	BETA-518966	AMS	Organic sediment	−24.2	10,360 ± 30	12,390–12,055 BP	G&22
Patino Fan	AGRVIGN	BETA-596989		Organic sediment	−24	12,140 ± 30	14,107–13,870 BP	G&22
Patino Fan	FP148B	LTL-19618A	AMS	Organic sediment	n.d.	36,470 ± 571 BC	42,155–40,535 BP	ISPRA21
T13	DENTE-NICOLA	BETA-630864	AMS	Tooth collagen	−19.9	2,070 ± 30	170 BC-10 CE	This study
	TR03-SUOLO02	BETA-630861	AMS	Charred material	−24.8	160 ± 30	1,665–1,820 CE	This study
	TR03-PAL01	BETA-630859	AMS	Organic sediment	−23.4	4,350 ± 30	4,975–4,850 BP	This study
	TR03-CWPIZ	BETA-630858	AMS	Organic sediment	−23.8	2,310 ± 30	2,360–2,180 BP	This study
	NOR13-CW3	BETA-630849	AMS	Organic sediment	−23.4	5,510 ± 30	6,395–6,215 BP	This study
	NOR13-CW2	BETA-630848	AMS	Organic sediment	−23.4	4,920 ± 30	5,720–5,590 BP	This study
	NOR13-06	BETA-630847	AMS	Organic sediment	−24.2	2,920 ± 30	3,165–2,965 BP	This study
(T6)	MONT3	Beta209273	AMS	Organic sediment	−24.7	3,460 ± 430	3,840–3,530 BP	G&2018
Patino Fan	EC204	LTL-20116A	AMS	Organic sediment	n.d.	43,051 ± 1,545 BC	46,545–43,455 BP	ISPRA21
T14	CDC-01	BETA-630862	AMS	Charred material	−25	310 ± 30	1,488–1,650 CE	This study
Pielarocca	PLR-01	BETA-630863	AMS	Organic sediment	−24.3	3,480 ± 30	3,835–3,685 BP	This study
T15	TR05-PS01	BETA-630857	AMS	Organic sediment	−24.9	2,490 ± 30	2,725–2,465 BP	This study
T16	TR06-FA02	BETA-630860	AMS	Charred material	−23.2	850 ± 30	1,155–1,265 CE	This study

(unit 4). The AMS ages of these colluvia fall around half of the past millennium (1,435–1,625 CE; 1,395–1,445 CE), predating the colluvial wedge 3, which contains an age of 1,640–1,805 CE. Below the present-day pedogenetic horizon (1), the trench shows the brownish colluvium (unit 2) laid down over the aforementioned erosional surface that truncates units 4 and 4a. It contains detrital coal dated 1,220–1,280 CE, which is surely reworked from its parent material (Unit 4).

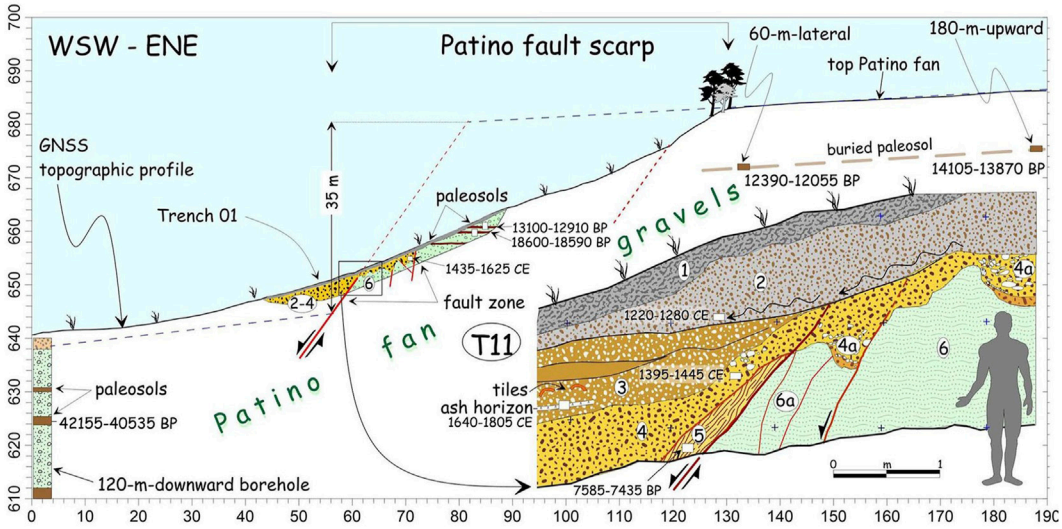

FIGURE 4
Section of the fault scarp where we opened Trench 11. Calibrated AMS dates of the sampled paleosols, charcoals, and organic colluvium are also shown. The bottom right is the paleoseismological log of the main fault zone. In this trench, we infer the occurrence of an event in modern times, characterized by a vertical offset of more than 1 m, definitely referable to the Mw 6.9 earthquake of January 14, 1703. Legend of stratigraphyc units: 1, present soil; 2, sandy-gravel colluvium; 3, sandy-gravel colluvial-wedge of the last surface faulting event; 4, sandy-gravel colluvium (4a gravelly infilling of man-made pits); 5, reddish sandy colluvium; 6, Late Pleistocene-Holocene Patino alluvial fan.

FIGURE 5
Photo-mosaic of the main fault zone in the north wall of Trench 11, cleaned and equipped with the metric grid. Bottom-right, whitish Patino fan gravels (Upper Pleistocene; 6 in Figure 4), tectonized and faulted against reddish colluvium (bottom-left; 5 in Figure 4), both mantled by other colluvia at the top (3-2 in Figure 4). Note the two pockets of coarse gravels dug into the Patino fan gravels (4a in Figure 4).

4.1.2 Tectonics and paleoseismology

The topographic leveling of the whole fault scarp allowed us to quantify, in this study, the vertical separation at ca. 35 m, which is the maximum value reached along the whole scarp facing Norcia. This offset cumulated progressively after the burying of the paleosols in the footwall, which were both found in the trench (18–12 ka) and even in surrounding outcrops (14–12 ka, Galli et al., 2022) few meters below the top surface (Figure 4). This suggests a slip-rate of ~2.5 mm/yr in this fault sector although the lack of correlative paleosols in the hanging wall hampers the absolute offset determination.

At the middle height of the scarp, a sharp N170°-striking and ~55°-dipping contact between the fan gravel (unit 6) and its colluvium (unit 4) is interpreted as the main fault plane (Figures 4, 5). The fault downthrows the fan gravel at least 5 m below the ground surface, which is the maximum depth reached by the digger without finding the gravel.

Considering the scarp steepness (35°–20°), the aforementioned zone of strong disturbance above the main fault is interpreted as due to coseismic gravity movements triggered by the main fault rupture. The downthrown of the hanging wall and the consequent relaxation in the footwall deposits resulted in the opening of wide fractures in the loose alluvial fan gravels, rapidly filled by reddish colluvia sliding downward from the above pedogenic layers. Charcoal collected in these faulted and remobilized deposits gave a calibrated age (1,435–1,625 AD; Figure 4), attesting to the very recent activity of the fault.

The paleoseismological analysis of the main fault zone provided some interesting indications regarding the last activations of the Norcia fault. In the fault gauge, we distinguished a reddish colluvium stretched and dragged along a fault (unit 5 in Figure 4). It could likely be an old colluvial wedge trapped and dragged between two fault branches that formed successively. Its AMS age (7.5 ky BP) could slightly predate an ancient surface faulting event. Above this, unit 4 is also faulted and dragged along the fault plane by at least 1 m. The space created by the coseismic down-throwing of unit 4 was quickly refilled by a wedge-shaped colluvial body made of fine gravels in a reddish, sandy-silty matrix (unit 3 in Figure 4). This contains tile fragments, detrital coals, and a peculiar 1-to-5-cm-thick level of wood-ash, which was recognizable all along the entire length of the trenched hanging wall. The AMS age of this level (1,640–1,805 CE) postdates Unit 4 faulting and unquestionably indicates that the responsible event is that of 14 January 1703.

FIGURE 6
The view of the southern wall of trench 13, cleaned and equipped with the metric and semimetric grid. From the right, a first subvertical fault lowers the cemented Patino gravels (8 in Figure 7), as does a second shear plane that faults these gravels against others in a reddish sandy matrix (7 in Figure 7) and against a reddish paleosol (5 in Figure 7). Upward, an anthropic erosional surface levels both footwall and hanging-wall, being buried by 0.7 m of fill and/or pedogenized agricultural soil at the top.

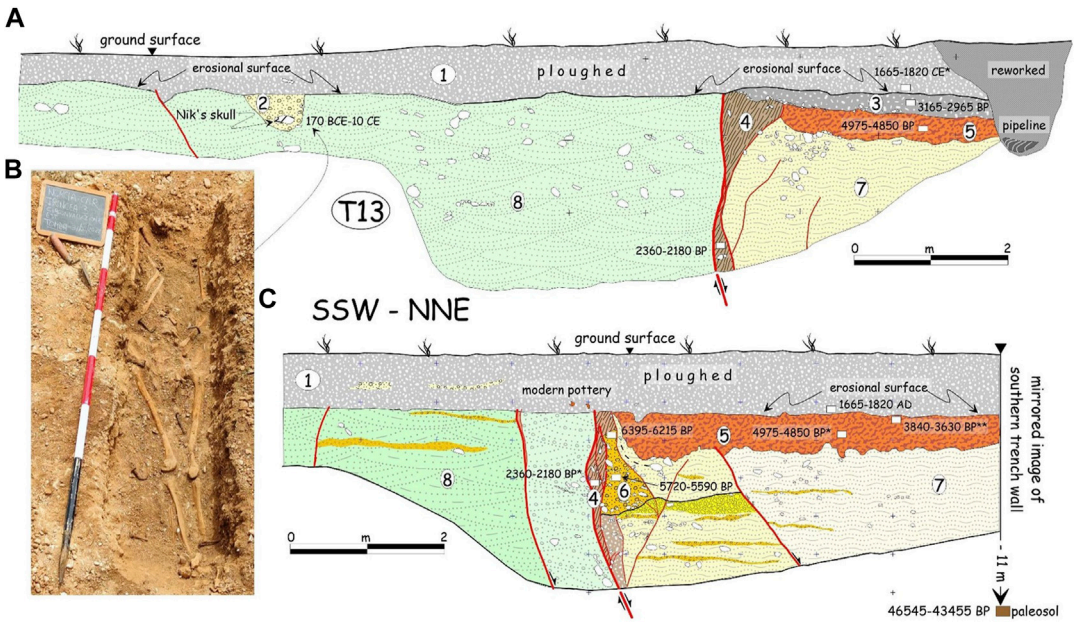

FIGURE 7
Paleoseismological sketches comparing the two walls of Trench 13. For convenience, the southern wall **(C)** has been mirrored. Given the obliquity with which the trench intersects the fault, the fault is more advanced in the northern wall **(A)** than in the southern wall. Besides the 1703 event, here, we hypothesize the presence of two previous events (*, a sample collected in the other trench wall; **, a sample collected in trench T6 in Galli et al., 2018). **(B)** oblique view looking SSE of Nik's skeleton.

Possibly, the ash layer might be due to the collapses and related fires triggered by the earthquake.

4.2 Trench 13 (Norcia antithetic splay)

Trench 13 was designed across the antithetic splay that, together with the synthetic one, gave rise to the Graben between the walled town and the Patino top surface (Figure 2). This structural saddle is both populated by modern buildings and reworked by large excavations and embankments that have housed containers and prefabs since the 1979 earthquake and again, since the 2016 earthquake. Where there were no housing blocks, the land surface was deeply leveled and reworked by centuries of agricultural and mining activity, predating even the building settlement. All of this has resulted in no scarp or surface evidence being associated

with the antithetic splay. Some indications of its subdued presence along the northwest continuation of the fault that Galli et al. (2005), Galli et al. (2018) trenched 500 m away are visible in the Electrical Resistivity Tomography (ERT) reported by Galli et al. (2018) and Peronace et al. (2022). The 40-m-long trench was opened in flat, uncultivated terrain to a depth of 3 m. Due to local impediments, it crossed the fault line obliquely, resulting in a 3-m-offset of the fault intersections on the two facing walls (Figures 6, 7). It is worth noting that next to the fault was found the burial site of a 1.8-m-tall man inside a wooden coffin secured by a dozen large iron nails. At the time of discovery, the skeleton was perfectly preserved, and the bones showed no fractures, except in the skull which appeared to be smashed.

4.2.1 Stratigraphy

In the footwall, the excavation exposed mainly the well-stratified gravels of the Patino alluvial fan (Unit 8). In past centuries, these gravels had been extensively subjected to mining to a maximum depth of 1.5 m from the present ground level. The resulting pits were then filled by natural colluviation of surface deposits and mainly by loose, coarse, rounded gravels, within which numerous fragments of tiles, bricks, and coarse pottery of the modern age were found (outer sector of Figures 6, 7). Loose gravels in an orange silty-sandy matrix were found in the hanging wall (unit 7; upper portion of unit 8), covered by an orange silty-sandy, stiff paleosol with scattered flint clasts and ghosts of carbonate clasts (unit 5). The northern wall had an additional grayish layer above the orange paleosol, composed of reworked hardened sands with carbonate clasts and pottery fragments, likely fill material deposited for leveling a ground step (unit 3). Against the fault plane, colluvial wedges and a fracture fill were dragged and stretched along it (units 6, 4).

The succession was dated from seven AMS samples and through some correlations with similar deposits already dated in previous studies (Galli et al., 2018). In general, the Patino gravels, both of the footwall and hanging wall, were definitely deposited in the second half of the Upper Pleistocene, as shown by some ISPRA (2021) radiocarbon dating of paleosols intercepted at 10 m below the ground surface in geognostic boreholes (i.e., ~45 ka). As for the mature orange paleosol (unit 5), it was found in earlier trenches around Norcia, where its base was dated ~13.5 ka and its top was ~3.7 ka (Galli et al., 2018). In Trench 13, the age was that referable to a truncated portion of the paleosol (charcoal dated 4,975–4,850 BP). The overlying grayish layer in the northern wall (Unit 3, reworked fill material) provided a bulk age (3,165–2,965 BP) inconsistent with the deposition of the unit, which is historic, also given the presence of brick and tile fragments, as well as pottery shards. The radiometric age likely belonged to its parent material. A further chronological constraint came from the buried man (northern wall, unit 2), whose AMS age was found to be late-Republican, between the early second century BCE and the beginning of the present era (170 BCE-10 CE). The inhumation and last surface faulting were sealed by the uppermost deposit (unit 1), which contained a detrital charcoal of the modern age (1,665–1,820 CE), besides modern pottery shards and fragments of bricks and tiles.

4.2.2 Tectonics and paleoseismology

The good stability of the trench allowed for a comparative paleoseismological analysis of the two walls. The fault abruptly displaced the lightly cemented Patino gravels (unit 8), down-throwing them under the bottom of the trench and against the upper outcropping portion of a similar gravel succession (unit 7). The latter was covered by the orange paleosol (unit 5), which had been completely eroded in the footwall (Figures 6, 7). In both walls, brownish-red colluvium (unit 4) was stretched and dragged down to the bottom of the trench along the main shear plane. It might have been the fill of an open fracture near the fault or, likely, the ghost of a colluvial wedge, as seen in the northern wall, where its upper part had preserved the shape of a wedge. Its age (2,360–2,180 BP) could have predated an ancient surface faulting event.

In addition to this colluvium, an older, deformed colluvial wedge was clearly visible in the southern wall, providing a basal age of 5,720–5,590 BP and an upper age of 6,395–6,215 BP. As is often the case, when a fault step is formed at the surface, the first deposit to fall over the scarp is the higher and younger one, followed by the older one below. It is therefore conceivable that the younger age was closer to the faulting event that generated this colluvial wedge, predating it.

In summary, the presence of trapped, faulted, and dragged colluvial wedges along the fault plane and their geometric relationships with the orange paleosol and overlying deposits allow us to hypothesize a sequence of surface faulting events. The last one occurred well after 170 BCE-10 CE when the top of the cemented gravels was excavated for the burial of the Roman man, but shortly before 1,665–1820 CE, a time immediately following anthropic leveling/plowing of the coseismic scarp (Unit 3). As already seen in Trench 11, this is obviously referable to the 14 January 1703 event. The penultimate event probably occurred just before the formation of the colluvial wedge dated 2,360–2,180 BP that was subsequently dragged along the fault by the successive, 1703 earthquake. Considering that this age belongs to the parent material of the colluvial wedge, it predates the earthquake, probably that of 99 BCE. A very suggestive hypothesis is that this earthquake has something to do with the death of the man with the smashed skull, who lived in the first-second century BCE. We do not know whether his burial near the fault had apotropaic significance, but his traumatic death and the well-known earthquake of 99 BCE could all be pieces of the same puzzle.

Finally, an older event could be evidenced by the faulted colluvial wedge present in the southern wall, which can be dated post 5,720–5,590 BP, the age of its parental material, and ante 4,975–4,850 BP, the age of the orange paleosol covering the wedge itself.

4.3 Trench 14 (Capo del Colle)

Following the 2016 earthquakes in central Italy (Mw 6.6), the demolition of heavily damaged buildings in the settlement of Capo del Colle (cdc in Figure 1) uncovered the Campi Fault slickenside just beneath the foundations of an 18th-century tenement house. Here, we opened a trench flush with the remaining wall of this house and above the slickenside (Figure 8). Considering the historical stratigraphy, this excavation offered a superior alternative to what an ordinary trench would have provided. The excavation was made along a rubble masonry wall that was preserved in elevation for a height of 1–2 m and a length of 6–7 m and provided detailed information on the last surface rupture of the fault.

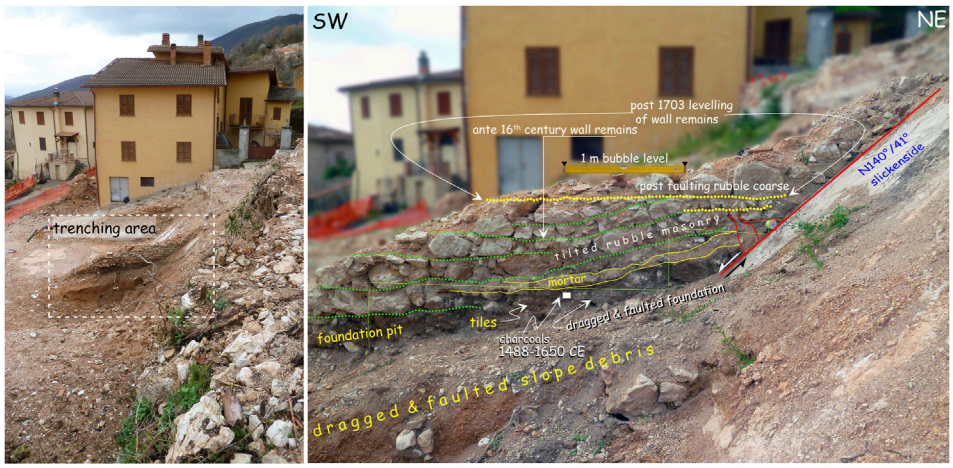

FIGURE 8
Line drawing of the Capo del Colle trench, showing the deformation of a 16th-century house foundation because of the Campi fault slip in 1703 (see the sketch in Figure 9). The house remains were successively cut and leveled in order to build a new house in the 18th century that was demolished after the 2016 earthquake.

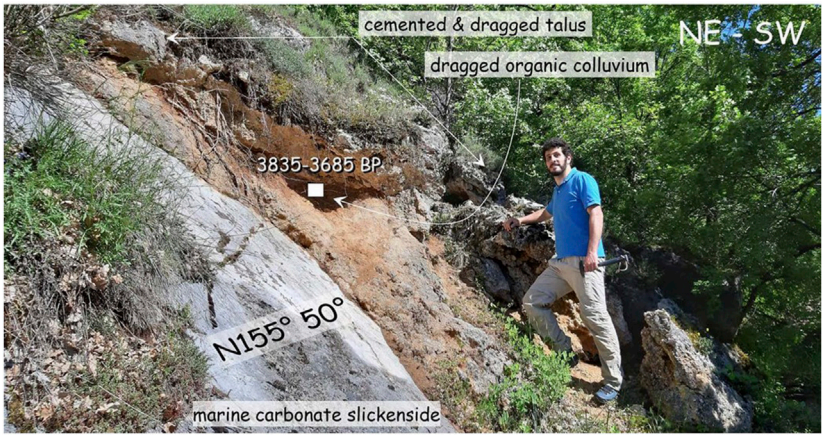

FIGURE 9
Outcrop along the Campi fault segment where cemented slope debris is faulted and dragged along the carbonate slickenside. A sandy organic colluvium, embedded in this debris and involved in the faulting, provided a Late Holocene 14C age.

It is worth noting that in addition to the study of this site, the Late Holocene fault activity was confirmed also southeast of Capo del Colle, near the village of Pielarocca, where slope deposits dated 3,835–3,685 BP were dragged and faulted along the same slickenside seen in Capo del Colle (Figure 9).

4.3.1 Stratigraphy

Demolition work carried out by firefighters exhumed the foundation of the wall of a house made of roughly squared limestone blocks, which shows evidence of ductile and brittle deformation as well as caesuras, restorations, and reconstructions (Figures 8, 10). In the hanging wall, we excavated flush with the wall foundation, finding irregular limestone blocks (unit 2) embedded in the foundation ditch (unit 4). The ditch, in turn, was originally dug into weakly cemented slope debris (unit 5). In the footwall, the ditch and the foundation blocks appear to rest directly above the carbonate slickenside (unit 6). Below the stone foundation, a mortar horizon (3) overlies the top of the ditch, which in turn contains brick and tile fragments and charred materials. Within the ditch, detrital charcoal dated 1,488–1,650 CE predates the construction of the first house, as also suggested by some reused 16th-century architectural elements that survived later destructions (e.g., marble window frames; F. Iambrenghi, oral communication).

4.3.2 Tectonics and paleoseismology

The wall remains and its foundation, leaning directly on the carbonate slickenside of the Campi fault, show evidence of the

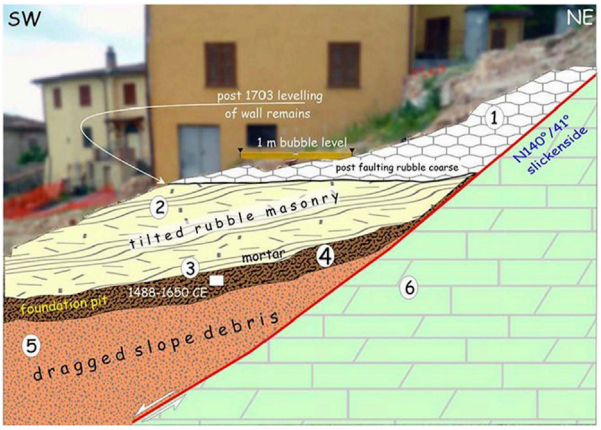

FIGURE 10
Sketch of the faulted 16th-century house. 1, remains of the post-1703 house masonry; 2, remains of the deformed 16th-century house (foundation and wall); 3, mortar level topping the foundation ditch (4); 5, slightly cemented slope debris; 6, Mesozoic carbonates.

FIGURE 11
View overlooking NE of the eastern wall of trench 15. The homogeneous, alluvial-fan gravel deposition is interrupted only by a truncated paleosol. Its apparent warping could account for a coseismic deformation that occurred after the last centuries BCE.

deformation undergone during one coseismic slip of the fault, resulting in the dragging of the ditch infill material over the slickenside and the tilting of the coursed stone masonry (Figures 8, 10). Following this destructive event, in order to build a new masonry wall in unconformity over the previous one (i.e., with horizontal regular courses; unit 1), the remains of the tilted/faulted wall were cut and leveled horizontally with smaller stones. As the first house was built in the 16th century, its destruction and subsequent reconstruction are again attributable to the earthquake of 14 January 1703, the only event the magnitude of which is consistent with surface rupture.

4.4 Trench 15 (Campi-Capo del Colle)

Trench 15 was designed in the sector between Capo del Colle and Campi (Figure 1) on the basis of geomorphological indications that were strengthened by geoelectrical investigations (ERT in Peronace et al., 2022). In this sector, the fault was buried by a thick nail of slope debris and alluvial fan deposits coming from three deep valleys carved across the rocky hillslopes. The selected site presented a subdued scarp crossing the apex of an alluvial fan, matching at a depth with lateral contact between terrains with different resistivities in the ERT sections. The trench was 45-m-long and 3-m-deep at an elevation between 830–820 m above sea level (Figure 11).

4.4.1 Stratigraphy

Throughout its length, the trench exposed a homogeneous succession of fine, alluvial fan gravels, well-stratified (Figure 11), invert-graded, subangular, and reworked upward by agricultural processes. A few anthropic pits filled with angular stones interrupted the lateral continuity of the gravel strata. Approximately 1.5–1.8 m below the earth ground, we individuated a 0.3–0.5-m-thick paleosol, truncated, and buried at the top by fan gravel sheets (Figure 11). On the western side of the trench, the fan gravels eroded completely the paleosol, resting directly on the gravels below. The paleosol was sampled and dated to 2,725–2,465 BP (775–515 BCE), a time likely reflecting a wetter and more stable climate in the first half of the first millennium BCE.

4.4.2 Tectonics and paleoseismology

As suggested also by the ERT analyses at depth (in Peronace et al., 2022) and by the faint flexure at the surface, the paleosol, which parallels the ground surface in the first 30 m of the trench, shows a flexure and an appreciable thickening going downward. However, this is not associated with any certain element of either brittle or ductile deformation in the surrounding gravels, making it hard to interpret whether the flexure is due to tectonics or is the product of several phases of fan accretion before and after the soil development. If it were tectonic, then the event or the events occurred during and/or after the paleosol deposition, i.e., 2,725–2,465 BP, a time which matches both the 99 BCE and the 1703 earthquakes.

4.5 Trench 16 (Campi basso)

Trench 16 was designed across the trace of the Campi fault, a hundred meters east of the limestone hill where the medieval settlement of Campi stands (Figure 1). The trench was opened at the apex of the alluvial fan coming from a deep valley carved in the rocky hillslope at an elevation of 760–750 m above sea level. The 65-m-long excavation intersected two uncultivated fields separated by an anthropic scarp having the same strike as the fault trace (Figure 12) and also matching an 80-m-deep ERT indication, i.e., a lateral contact between deposits with different resistivities (in Peronace et al., 2022). Here it appears that humans have always used a pre-existing tectonic escarpment as a field boundary, making a much higher escarpment for cultivation needs. The depth of the trench north of the scarp was 2–3 m, while south, it required

FIGURE 12
Drone view of trench 16, opened in the apex of an alluvial fan near Campi. The anthropic scarp in the foreground is where we have found faint indications of faulting of the fan gravels succession.

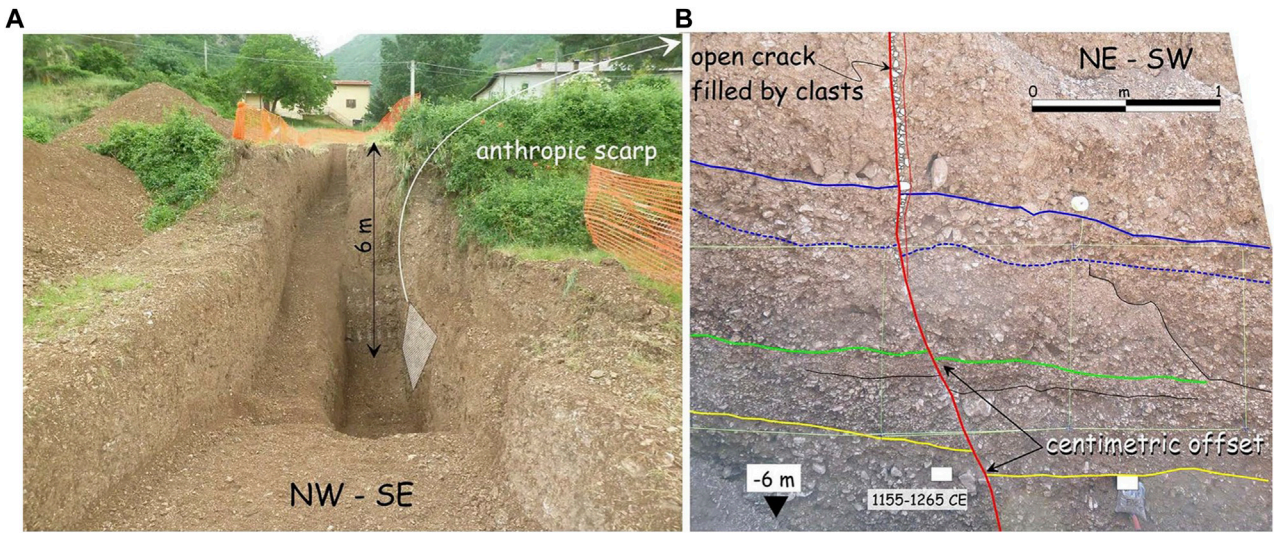

FIGURE 13
(A) view overlooking NE of the telescopic trench 16. **(B)** the detail of the deepest portion of the SE wall showing the offset of the fan-gravel layers that occurred after the 13th century CE.

deepening down to 6 m from ground level and grading on the northern side (Figure 13). As in the previous case, the master fault does not outcrop on the hillslopes below Campi, and thus we based trench siting just on the match between the scarp and the ERT clues.

4.5.1 Stratigraphy

Throughout its length and depth, the trench exposed a homogeneous succession of faintly stratified, medium-to-fine alluvial fan gravels, with angular clasts, alternating with discontinuous, massive coarse horizons in a brown sandy-silty matrix. Here too, as everywhere, there are anthropic spalling pits at various depths, filled with loose coarse gravels, representing a source of wall instability, such as requiring wall grading (Figures 12, 13). The monotonous succession of inverse-graded layers continues at a depth even in the section where deepening of the trench bottom was conducted down to approximately 6 m from the ground level. At the trench bottom, a level with organic materials predates the entire exposed succession to 1,155–1,265 CE, testifying to the high rate of sedimentation occurring near the apex of the fan (6 m in less than 800 years; i.e., 8 mm/y), which is almost an order of magnitude higher than the slip rates of the Apennine faults.

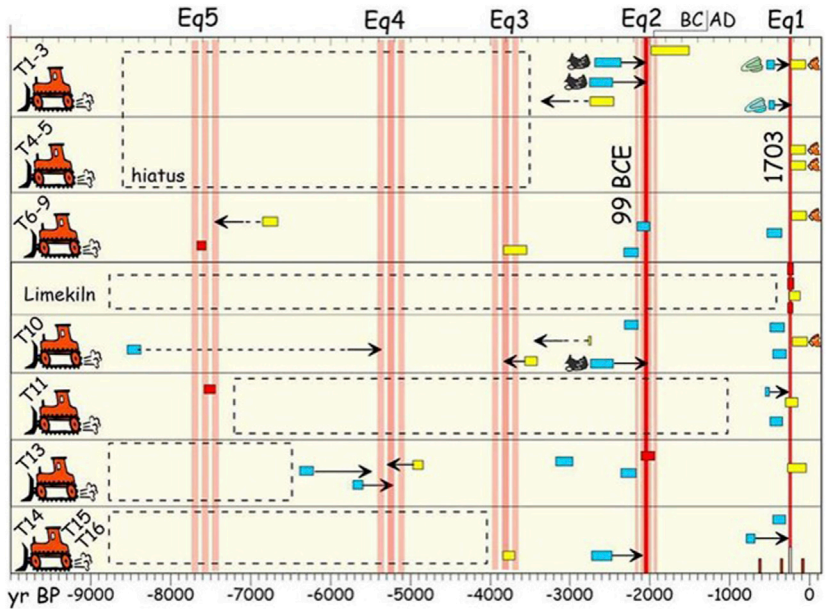

FIGURE 14
Chronogram of the surface rupture events identified from within trenches. Colored horizontal bars represent key dated samples that bracket the different earthquakes (2σ calibrated interval for 14C ages). Tones suggest *ad quem* (red), *post quem* (cyan), and *ante quem* (yellow) terms. Archaic age pottery (black), renaissance pottery (green), and modern pottery (orange) are also shown, together with their time-span bar. Horizontal arrows point to the assumed paleoevent age (dashed if related to uncertain indication). Vertical pink bars suggest the most probable earthquake interval (Eq1-5), as deduced from the samples' age and considering the nature of the surrounding deposits (see text for further details). The little vertical bars (bottom right) indicate the four historical earthquakes that were likely sourced by the Norcia fault (Figure 4), being too small to leave indications within the deposits explored in the trenches. Dashed rectangles suggest stratigraphical hiatuses.

4.5.2 Tectonics and paleoseismology

Next to the anthropic scarp, and at the ERT anomaly seen in-depth, on the eastern wall of the trench, we observed a subvertical alignment of en-echelon clasts filling an open crack in the gravel layers Here, we decided to widen the trench and deepen the excavation to the maximum length of the excavator boom, also creating a safety step on the north wall (Figure 13). In the newly deepened wall, at a depth of approximately 3 m, the subvertical crack evolves into a 70° dipping shear plane, with an increasing displacement of the gravel layers downward (15 cm at the bottom of the trench). The dating of the organic matrix of the deepest level of the alluvial fan (1,155–1,265 CE) provides the terminus post quem of the overlying deformation. As in previous cases, it is likely that this displacement is related to the surface rupture of the 14 January 1703 earthquake, which occurred likely on a secondary splay.

5 Resulting paleoearthquake recurrence and relationship with the Mt vettore fault

Considering the results obtained in the previous urban-splay trenches (Galli et al., 2005; Galli et al., 2018), those from the limekiln on the Norcia master fault (Galli et al., 2022), those from the excavations on the Mt Alvagnano and Cascia faults (Galli et al., 2020), and those presented in this paper, we feel like proposing a succession of five consecutive paleoearthquakes sourced by the whole NFS since the Middle Holocene. Our hypothesis is founded on more than 50 14C datings of samples collected along the entire NFS, each constituting as much as ante-ad-post quem terms for every surface faulting event.

Given the length of the NFS and the empirical laws relating surface length to magnitude (e.g., Wells and Coppersmith, 1994; Galli et al., 2008; Wesnousky, 2008; Leonard, 2010), and especially the macroseismic magnitude assigned to the 1,703 event (Graziani et al., 2022), we assume that all five events (or seismic sequences, which are impossible to detect with paleoseismological techniques) were characterized by approximately the same magnitude (Mw ~ 6.9). We also assume that the other historical Mw ~ 6 events we have attributed to segments of the NFS were not associated with a fault slip large enough to reach the surface and/or be visible in the trenches. Due to sedimentary hiatuses and/or erosive episodes, the five events are not visible in all the trenches, except the ultimate and the penultimate which have been recognized in all the studied sites (eq1 and eq2 in Figure 14). It is also possible that in some earthquakes, the individual secondary splays did not rupture at the surface or did so with such a small offset that it was not recorded in the stratigraphic succession. The ultimate (Eq1), whose surface faulting was also described by coeval witnesses, is certainly the 14 January 1703 earthquake, which was visible and well datable in all trenches and exposures of all the segments both along the master faults and on the secondary splays. The penultimate event (Eq2) is visible in almost all the urban splays and the Campi segment, with an age bracketed around the 99 BCE earthquake.

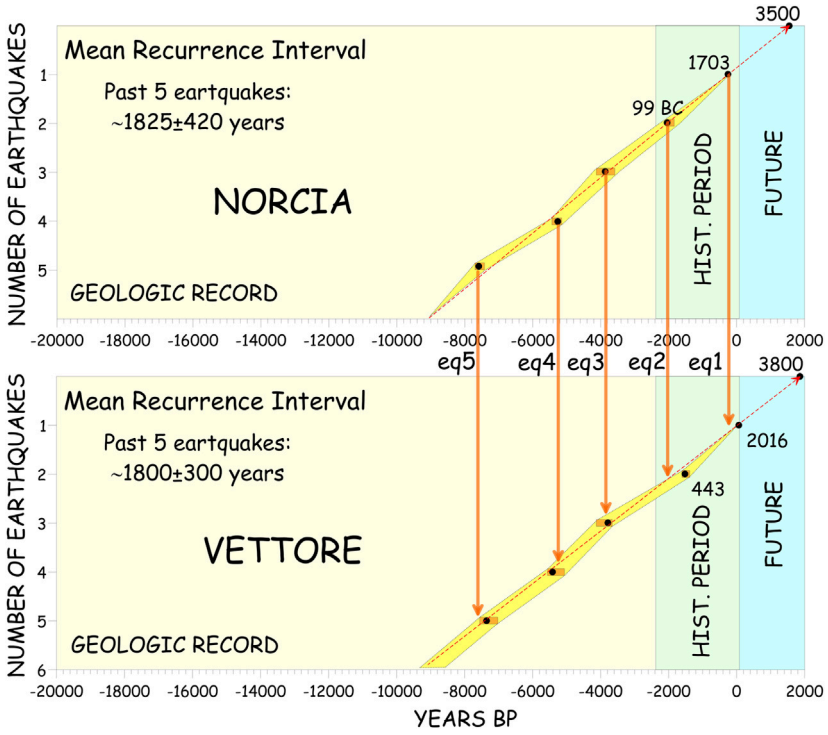

FIGURE 15
Comparison between the sequence of the five paleoearthquakes sourced by the Norcia and Mt Vettore fault systems. There seems to be a kind of synchronism between the two faults, albeit with a short secular lag between each earthquake originating in the two systems, with the Norcia faults anticipating and perhaps triggering the Monte Vettore ruptures (updated and modified from Galderisi and Galli, 2020). The yellow area represents the ^{14}C range of key samples constraining every surface rupture.

The three previous events have been recognized only in some trenches and in some segments. However, the age of the oldest (Eq5) is well constrained by two ad quem terms (7.6–7.4 ka), whereas the successive, poorly constrained one (Eq4) is recognized only by a pair of post and ante quem terms (around 5.2 ka). The intermediate event between the historical and the prehistorical ones (Eq3) has only ante quem terms that suggest an approximate age of 3.8 ka. With respect to the results in Galli et al. (2018), here, we strengthened the dating of all the events and discovered a new one that bridges the previously existing gap between the paleoearthquakes that occurred around 3.8 and 7.6 ka (Eq4 in Figure 14).

The recurrence time for these paleoearthquakes during the Middle Holocene was 1,825 ± 420 years, with an elapsed time since the last event of 320 years. However, in terms of seismic hazard, if we consider only the period that began in 1328 CE and all the aforementioned Mw ~ 6 earthquakes, all of which were strong enough to cause damage and casualties, the recurrence time for this class of magnitude is 130 ± 90. Both should be taken into account in risk mitigation procedures.

Finally, we emphasize an interesting relationship existing between the two parallel NFS and MVFS (Figure 1), which was already noted by Galli et al. (2019). Thanks to several paleoseismological trenches, we know that even the MVFS generated several 2016-like events since the Middle Holocene, with recurrence times similar to those of the NFS (i.e., 1,800 ± 300 years; Galli et al., 2019). Since we now have a more reliable and complete knowledge of NFS palaeoearthquakes over the last 8 ka, we can better compare the occurrence of palaeoearthquakes between the two fault systems. In agreement with Galderisi and Galli (2020), it appears that the NFS earthquakes preceded the Monte Vettore earthquakes by a few centuries, albeit within the error bar of the palaeoseismological method (yellow area in Figure 15; i.e., ^{14}C range of key-samples constraining every surface rupture).

In historical times, the NFS ruptured in 99 BCE, followed by the MVFS in 443 CE, whereas the NFS ruptured again in 1703, followed by MVFS in 2016. At the beginning of the Late Holocene, the NFS ruptured at approximately 3.8 ky BP, at approximately the same time as the MVFS (4.1–3.9 ky BP). During the Middle Holocene, the NFS ruptured at approximately 5.2 ky BP, while the MVFS ruptured around 5.3–5.0 ky BP. Earlier, the NFS ruptured at approximately 7.6–7.4 ky BP, as well as the MVFS (7.6–7.4 ky BP). Bearing in mind that the dating of paleoseismic events often have large associated errors or large time intervals within which earthquakes are bracketed (Galli et al., 2008; McCalpin, 2009), it does indeed appear that the two fault system ruptured closely to each other during the Holocene. According to Galderisi and Galli (2020), this could be due to Coulomb stress transfer (CST) deep into the seismogenic volume of the Mt Vettore hanging wall following each NFS rupture, which instead does not happen when it is the MVFS that ruptures.

Recent faults interaction following CST on other active normal faults of central Apennines is proposed by Mildon et al. (2017), who focused on the 1997–2009–2016 seismic sequences of central

Apennines, whereas Wedmore et al. (2017) analyzed how coseismic CST may have altered earthquake return times in central Apennines in the past seven centuries. From this point of view, we hope that our data might be useful in future studies concerning fault interaction, strain storage, and dynamic topography like those already published for the central Italian Apennines on selected faults (Mildon et al., 2022).

6 Conclusion

We dug five new paleoseismological trenches across the Norcia fault system, which consists of three main normal segments running for more than 30 km along the central Italian Apennine divide. Results complement and strengthen those already collected in 10 previous trenches opened over the past 20 years across the two urban splays crossing the Norcia town outskirts and from outcrops excavated along the Norcia and Cascia-Mt Alvagnano master faults. In addition to two new trenches through the Norcia urban splays, here, we present data from three trenches along the previously uninvestigated Campi segment.

We have identified five paleoearthquakes that occurred in the last 8 ka, which we hypothesize to be very similar to the 14 January 1703 earthquake (Mw 6.9). In addition to the 1703 event, we found evidence for a Roman earthquake, probably from 99 BCE, attested in Norcia from historical records, and three previous earthquakes that occurred around 3.8, 5.2, and 7.5 ky BP. Our interpretation is based on more than 50 AMS dating of key samples (coals, paleosols, organic sediments, bones, and teeth), combined with archaeological determinations of pottery shards. The resulting recurrence time for 1703-like events is fairly regular (1,825 ± 420 years), with an elapsed time since the last event being 320 years.

However, in terms of seismic hazard, considering that the Mw ~ 6 earthquakes generated in historical times by segments of the NFS have always caused casualties and damage, one should also consider the return time for this class of events, which is much shorter, 130 ± 90 years.

By comparing the paleoseismic histories of the Norcia and Mt Vettore faults system, we realized that there would seem to be some synchronism between the two faults in the past 8 ka, albeit with a possible, short secular lag between each earthquake originating in the two structures, with the Norcia faults anticipating and perhaps triggering the Monte Vettore ruptures. This kind of faults conversation, tentatively attributable to Coulomb stress transfer from the Norcia to the Mt Vettore fault, would deserve further investigation.

Data availability statement

All data are presented in the paper and further information can be requested directly from the authors.

Author contributions

PG and EP conceived the project, acquired the funding, and participated in all aspects of the fieldwork. PG wrote the manuscript. PM participated in the fieldwork. II and FP participated in the trenches survey. EP and FP participated in editing the manuscript. All authors contributed to the article and approved the submitted version.

Funding

Trenching was supported by the Istituto Nazionale di Geofisica e Vulcanologia of Rome, on behalf of the Commissaro Straordinario alla ricostruzione Sisma 2016, aimed at the "Redefinition of the Attention Zones for the Active and Capable Faults that emerged from the seismic microzonation studies carried out in the municipalities affected by the seismic events that occurred on 24 August 2016" (CUP D58I20001090001).

Acknowledgments

We are grateful to all the people of Norcia who have supported and endured us all these years. We thank the owners of all the fields where we dug our trenches and E. Lucci for his logistic support and bulldozing skill. We are grateful to Eng. Fabio Iambrenghi for his professional support in the Capo del Colle site. Criticisms of A.M. Michetti, M.F. Ferrario and Y. Aoki strongly improved the final version of the ms. The view and conclusion contained in this paper are those of the authors and should not be interpreted as necessarily representing the official policies, either expressed or implied, of the Italian Government.

Conflict of interest

The authors declare that the research was conducted in the absence of any commercial or financial relationships that could be construed as a potential conflict of interest.

Publisher's note

All claims expressed in this article are solely those of the authors and do not necessarily represent those of their affiliated organizations, or those of the publisher, the editors and the reviewers. Any product that may be evaluated in this article, or claim that may be made by its manufacturer, is not guaranteed or endorsed by the publisher.

References

Baglivi, G. (1710). *Historia Romani terraemotus, and urbium adjacentium, anno infelicissimo 1703*. Lyon: Opera omnia medicopratica, et anatomica, 523–533.

Blumetti, A., and Dramis, F. (1993). Il Pleistocene inferiore nell'area nursina. *St. Geol. Cam., Spec. Issue* 1992 (1), 55–64.

Blumetti, A. M. (1995). "Neotectonic investigation and evidence of paleoseismicity in the epicentral area of the January–February 1703, central Italy, earthquakes," in *Perspectives in paleoseismology*. Editors L. Serva and B. Slemmons (United States: Special Publication-Association of Engineering Geologists), 83–100.

Boncio, P., Lavecchia, G., and Pace, B. (2004). Defining a model of 3D seismogenic sources for seismic hazard assessment applications: Thecase of central Apennines (Italy). *J. Seismol.* 8 (3), 407–425. doi:10.1023/B:JOSE.0000038449.78801.05

Bosi, C., Galadini, F., Giaccio, B., Messina, P., and Sposato, A. (2003). Plio-Quaternary continental deposits in the Latium-Abruzzi Apennines: The correlation of geological events across different intermontane basins. *Italian J. Quat. Sci.* 16, 55–76.

Brozzetti, F., and Lavecchia, G. (1994). Seismicity and related extensional stress field: The case of the Norcia seismic zone (Italy). *Ann. Tect.* 8, 36–57.

Calamita, F., Coltorti, M., Deiana, G., Dramis, F., and Pambianchi, G. (1982). Neotectonic evolution and geomorphology of the Cascia and Norcia depression (Umbria–Marche apennine). *Geogr. Fis. Din. Quat.* 5, 263–276.

Calamita, F., Coltorti, M., Farabollini, P., and Pizzi, A. (1994). Le faglie normali quaternarie nella dorsale appenninica umbro-marchigiana: Proposta di un modello di tettonica di inversione. *St. Geol. Cam., Spec. Issue* 1994 (1), 211–225.

Calamita, F., Pizzi, A., Romano, A., Roscioni, M., Scisciani, V., and Vecchioni, G. (1995). La tettonica quaternaria nella dorsale appenninica ummbro-marchigiana: Una deformazione progressiva non coassiale. *St. Geol. Cam., Spec. Issue* 1995 (1), 203–223.

Cello, G., Mazzoli, S., Tondi, E., and Turco, E. (1997). Active tectonics in the central Apennines and possible implications for seismic hazard analysis in peninsular Italy. *Tectonophysics* 272 (1), 43–68. doi:10.1016/S0040-1951(96)00275-2

Cinque, A., Patacca, E., Scandone, P., and Tozzi, M. (1993). Quaternary kinematic evolution of the Southern Apennines. Relationship between surface geological features and deep lithospheric structures. *Ann. Geofis.* 36 (2), 249–260.

Coarelli, F., and Diosono, F. (2009). *I templi e il forum di Villa S. Silvestro. La Sabina dalla conquista romana a Vespsiano*. Roma: Edizioni Quasar.

D'Agostino, N. (2014). Complete seismic release of tectonic strain and earthquake recurrence in the Apennines (Italy). *Geophys. Res. Lett.* 41, 1155–1162. doi:10.1002/2014GL059230

De Carolis, P. (1703). in *Relazione generale delle ruine, e mortalità cagionate dalle scosse del Terremoto de' 14. Gennaro e 2. Febbraro 1703 in Norcia, e Cascia, e loro contadi (omissis)*. Editor L. A. Chracas (Roma: Edizioni Quasar), 27.

De Carolis, P., and Franceschini, A. (1703). *Ragguaglio delle mine e precipitio causate in Cascia e ne suoi 50 castelli dal terremoto delli 14 di Gennaro del 1703*. Roma: Archivio Comunale Cascia.

Delano, J., Briggs, R., DuRoss, C., and Gold, R. (2021). Quick and dirty (and accurate) 3D paleoseismic trench models using coded scale bars. *Seismol. Res. Lett.* 92, 3526–3537. doi:10.1785/0220200246

Devoti, R., D'Agostino, N., Serpelloni, E., Pietrantonio, G., Riguzzi, F., Avallone, A., et al. (2017). A combined velocity field of the mediterranean region. *Ann. Geophys.* 60 (2), S0215. doi:10.4401/ag-7059

Fazzini, P., Loschi, A. G., Maffei, M., Parea, G., Mercuri, A. M., Trevisan, M., et al. (2001). I depositi quaternari del bacino di Norcia, Atti e Memorie. *Acc. Naz. Sci. Lett. Arti Modena* 8 (3), 413–455.

Galadini, F., and Galli, P. (2000). Active tectonics in the central Apennines (Italy) e input data for seismic hazard assessment. *Nat. Hazards* 22, 225–268. doi:10.1023/a:1008149531980

Galadini, F., and Galli, P. (2003). Paleoseismology of silent faults in the central Apennines (Italy): The Mt. Vettore and laga mts. Faults. *Ann. Geophys.* 46, 815–836. doi:10.4401/ag-3457

Galadini, F., and Messina, P. (2004). Early-middle Pleistocene eastward migration of the abruzzi apennine (central Italy) extensional domain. *J. Geodyn.* 37, 57–81. doi:10.1016/j.jog.2003.10.002

Galderisi, A., and Galli, P. (2020). Offset components and fault-block motion during the 2016 central Italy earthquake (Mw 6.6, Monte Vettore fault system). *J. Struct. Geol.* 134, 104014. doi:10.1016/j.jsg.2020.104014

Galli, P., Galadini, F., and Calzoni, F. (2005). Surface faulting in Norcia (central Italy): A "paleoseismological perspective". *Tectonophysics* 403, 117–130. doi:10.1016/j.tecto.2005.04.003

Galli, P., Galadini, F., and Pantosti, D. (2008). Twenty years of paleoseismology in Italy. *Earth Sci. Rev.* 88 (1–2), 89–117. doi:10.1016/j.earscirev.2008.01.001

Galli, P., and Galadini, F. (1999). Seismotectonic framework of the 1997-1998 umbria-marche (central Italy) earthquakes. *Seismol. Res. Lett.* 70, 417–427. doi:10.1785/gssrl.70.4.417

Galli, P., Galderisi, A., Ilardo, I., Piscitelli, S., Scionti, V., Bellanova, J., et al. (2018). Holocene paleoseismology of the Norcia fault system (central Italy). *Tectonophysics* 745, 154–169. doi:10.1016/j.tecto.2018.08.008

Galli, P., Galderisi, A., Marinelli, R., Peronace, E., Messina, P., and Polpetta, F. (2020). A reappraisal of the 1599 earthquake in Cascia (Italian Central Apennines): Hypothesis on the seismogenic source. *Tectonophysics* 774, 228287–231016. doi:10.1016/j.tecto.2019.228287

Galli, P., Galderisi, A., Peronace, E., Giaccio, B., Hajdas, I., Messina, P., et al. (2019). The awakening of the dormant Mount Vettore fault (2016 central Italy earthquake, *M* w 6.6): Paleoseismic clues on its millennial silences. *Tectonics* 38, 687–705. doi:10.1029/2018tc005326

Galli, P., Giaccio, B., and Messina, P. (2010). The 2009 central Italy earthquake seen through 0.5 Myr-long tectonic history of the L'Aquila faults system. *Quat. Sci. Rev.* 29 (27-28), 3768–3789. doi:10.1016/j.quascirev.2010.08.018

Galli, P., and Molin, D. (2014). Beyond the damage threshold: The historic earthquakes of Rome. *Bull. Earthq. Eng.* 12, 1277–1306. doi:10.1007/s10518-012-9409-0

Galli, P., Peronace, E., and Messina, P. (2022). Archaeoseismic evidence of surface faulting in 1703 Norcia earthquake (central Italian Apennines, Mw 6.9). *Geosciences* 12 (1), 14. doi:10.3390/geosciences12010014

Galli, P. (2020). Recurrence times of central-southern Apennine faults (Italy): Hints from palaeoseismology. *Terra nova* 32 (6), 399–407. doi:10.1111/ter.12470

Galli, P. (2023). "Terremoti distruttivi a villa san silvestro, il contributo della paleosismologia," in *(a cura di), Villa San Silvestro di Cascia. Archeologia e storia di un abitato nella Sabina Montana dalla conquista romana al Medioevo*. Editor F. Diosono (Rome: Edizioni Quasar).

Giaccio, B., Galli, P., Messina, P., and Peronace, E. (2023). "Active or inactive? When the basin sediments unravel the status of activity of a fault," in 41st National Conference of the GNGTS, Bologna, Italy, 7-9 February, 2023 (IEEE).

Giaccio, B., Galli, P., Messina, P., Peronace, E., Scardia, G., Sottili, G., et al. (2012). Fault and basin depocentre migration over the last 2 Ma in the L'Aquila 2009 earthquake region, central Italian Apennines. *Quat. Sci. Rev.* 56, 69–88. doi:10.1016/j.quascirev.2012.08.016

Graziani, L., Rovida, A., and Tertulliani, A. (2022). The influence of cumulative intensity on macroseismic source parameters: The case of 2016–2017 and 1703 seismic sequences (central Italy). *Seismol. Res.Lett.* 20, 759–774. doi:10.1785/0220220038

Improta, L., Latorre, D., Margheriti, L., Nardi, A., Marchetti, A., Lombardi, A. M., et al. (2019). Multi-segment rupture of the 2016 Amatrice-Visso-Norcia seismic sequence (central Italy) constrained by the first high quality catalog of Early Aftershocks. *Sci. Rep.* 9, 6921. doi:10.1038/s41598-019-43393-2

ISPRA (2021). Note illustrative della Carta geologica d'Italia alla scala 1:50.000, foglio 337 Norcia. Available at: https://www.isprambiente.gov.it/Media/carg/note_illustrative/337_Norcia.pdf.

Leonard, M. (2010). Earthquake fault scaling: Self-consistent relating of rupture length, width, average displacement, and moment release. *Bull. Seismol. Soc. Am.* 100, 1971–1988. doi:10.1785/0120090189

Marsan, P., and Cerone, M. (1980). "Analisi degli effetti locali sui terreni," in *Analisi del comportamento dei terreni e delle costruzioni in muratura a seguito del terremoto del Settembre 1979 in Val Nerina* (Roma: CNR Progetto Finalizzato Geodinamica, ESA Editrice), 5–33.

McCalpin, J. P. (2009). *Paleoseismology*. 2nd Edition. Amsterdam-London: Academic Press, 615.

Mildon, Z. K., Roberts, G. P., Faure Walker, J. P., Beck, J., Papanikolaou, I., Michetti, A. M., et al. (2022). Surface faulting earthquake clustering controlled by fault and shear-zone interactions. *Nat. Commun.* 13, 7126. doi:10.1038/s41467-022-34821-5

Mildon, Z. K., Roberts, G. P., Faure Walker, J. P., and Iezzi, F. (2017). Coulomb stress transfer and fault interaction over millennia on non-planar active normal faults: the M w 6.5–5.0 seismic sequence of 2016–2017, central Italy. *Geophys. J. Int.* 210, 1206–1218. doi:10.1093/gji/ggx213

Peronace, E., Galli, P., Messina, P., and Polpetta, F. (2022). Accordo di Collaborazione scientifica CNR IGAG – INGV. Relazione tecnico scientifica fase 3 – lotto 1, comune di Norcia. Available at: https://sisma2016data.it/faglie/fase3/fase%203_norcia.zip.

Reitman, N. G., Bennett, S. E. K., Gold, R. D., Briggs, R. W., and DuRoss, C. B. (2015). High-resolution trench photomosaics from image-based modeling: Workflow and error analysis. *Bull. Seismol. Soc. Am.* 105 (5), 2354–2366. doi:10.1785/0120150041

Scarsella, F. (1941). *Carta geologica d'Italia, foglio 132, Norcia*. Roma: Regio Ufficio Geologico.

Sieberg, A. (1932). "Erdbeben," in *Handbuch der Geophysik* (Berlin: B. Gutenberg), 552–554.

Stucchi, M., and Albini, P. (2000). "Quanti terremoti distruttivi abbiamo perso nell'ultimo millennio? Spunti per la definizione di un approccio storico alla valutazione della completezza," in *Le ricerche del GNDT nel campo della pericolosità sismica (1996-1999)*. Editors F. Galadini, C. Meletti, and A. Rebez (Roma: CNR-GNDT), 333–343.

Stuiver, M., Reimer, P. J., and Reimer, R. W. (2021). Calib 8.2. Available at: http://calib.org.

Wedmore, L. N. J., Faure Walker, J. P., Roberts, G. P., Sammonds, P. R., McCaffrey, K. J. W., and Cowie, P. A. (2017). A 667 year record of coseismic and interseismic Coulomb stress changes in central Italy reveals the role of fault interaction in controlling irregular earthquake recurrence intervals. *J. Geophys. Res.* 122 (7), 5691–5711. doi:10.1002/2017jb014054

Wells, D. L., and Coppersmith, K. J. (1994). New empirical relationships among magnitude, rupture length, rupture width, rupture area, and surface displacement. *Bull. Seismol. Soc. Am.* 84, 974–1002. doi:10.1785/BSSA0840040974

Wesnousky, S. (2008). Displacement and geometrical characteristics of earthquake surface ruptures: Issues and implications for seismic-Hazard analysis and the process of earthquake rupture. *Bull. Seismol. Soc. Am.* 98 (4), 1609–1632. doi:10.1785/0120070111